Supplementary Materials for

Force dependence of filopodia adhesion: involvement of myosin II and formins

N.O. Alieva[1]†, A.K. Efremov[1,2]†, S. Hu[1], D. Oh[1], Z. Chen[1], M. Natarajan[1], H.T. Ong[1], A. Jégou[3], G. Romet-Lemonne[3], J.T. Groves[1,4], M.P. Sheetz[1,5], J. Yan[1,2,6], A.D. Bershadsky[1,7]*

correspondence to: alexander.bershadsky@weizmann.ac.il

This PDF file includes:

Other Supplementary Materials for this manuscript includes the following:

Materials and Methods

Cell culture and transfection

Hela-JW, a subline of a HeLa cervical carcinoma cell line derived in the laboratory of J. Willams (Carnegie-Mellon University) on the basis of better attachment to plastic dishes (*66*), was obtained from the laboratory of B. Geiger (*67*). The cells were grown in DMEM- Dulbecco's Modified Eagle Medium supplemented with 10% fetal bovine serum (FBS), 100 U ml^{-1} penicillin/streptomycin, 2 mM glutamine and 1 mM sodium pyruvate at 5% CO_2 at 37 °C. Cells were transfected with DNA plasmids by electroporation (two pulses of 1005 V for 35 ms) using Neon transfection system (Thermofisher). Expression vectors encoding the following fluorescent fusion proteins were used: GFP-myosin X (*37*) (gift from R. Cheney, University of North Carolina Medical School), tdTomato–Ftractin (*68*) (gift from M. J. Schell, Uniformed Services University, Bethesda, Maryland), myosin regulatory light chain (RLC)-GFP (*69*) (gift from W. A. Wolf and R. L. Chisholm, Northwestern University, Chicago, Illinois, USA), mCherry-Utrophin (*70, 71*), mCherry-VASP and mCherry-talin (M. Davidson collection, Florida State University, kindly provided by Dr. P. Kanchanawong). Reduced size myosin X construct (without 3'UTR) derived from GFP-myosin X was sub-cloned into mApple-C1 cloning vector backbone (M. Davidson collection, Florida State University). Full-length mDia2 was sub-cloned from GFP-C1-mDia2 (*72*) (gift from Dr S. Narumiya, Faculty of Medicine, Kyoto University, Japan) into mCherry-C1 vector. All cell culture and transfection materials were obtained from Life Technologies.

Live cell imaging and confocal microscopy

Following electroporation, cells were seeded at a density of 2×10^4 cells ml^{-1} in 2ml onto 35mm glass based dishes with 12 or 27 mm bottom base cover glass #1 in diameter (Iwaki, Japan) coated with 10 $\mu g\ ml^{-1}$ fibronectin (Calbiochem) for 20 min. Cells were imaged in Leibovitz's L-15 medium without Phenol Red containing 10% FBS at 5% CO_2 at 37 °C. Snapshot or time-lapse images were acquired with a spinning-disc confocal system (PerkinElmer Ultraview VoX) based on an Olympus IX81 inverted microscope, equipped with a 100× oil immersion objective (1.40 NA, UPlanSApo), an EMCCD camera (C9100-13, Hamamatsu Photonics), and Volocity control software (PerkinElmer). To perform structured illumination microscopy (SIM), dishes were mounted onto the observation chamber (CM-B25-1 Chamlide CMB chamber) of a Nikon Ti-E Motorised Inverted Microscope. The SIM images were taken with dual-color SIM mode (laser λ = 488nm and 561nm) using a 100× oil objective (1.49 NA) with autofocus maintained by the Nikon Perfect Focus system. The samples were mounted in a humidified cell culture chamber and maintained at 37 °C with 5% CO_2.

Transfection of siRNA and immunoblotting

Cells were seeded into a 35 mm dish on day 0 and transfected with 100μM of MYH9 ON-TARGET plus SMARTpool siRNA (L-007668-00-0005, Dharmacon) using Screenfect^{TM}A (WAKO, Japan) on day 1. Control cells were transfected with scrambled control ON-TARGET plus Non-targeting pool siRNA (D-001810-10, Dharmacon). Transfection of plasmid GFP-myosin X and tdTomato-Ftractin was performed in the evening of the day 1 using Jet Prime transfection reagent (Polyplus transfection, France)

and cells were imaged on day 2. For assessment of myosin IIA heavy chain expression, transfected cells were lysed in RIPA buffer on day 2 (exactly 24 hours following siRNA transfection) and analyzed by Western blotting with primary rabbit antibodies to the myosin IIA tail domain (M8064, Sigma-Aldrich, dilution 1:1000); staining of α-tubulin with monoclonal DM1A antibody (T6199, Sigma-Aldrich, dilution 1:5000) was used as a loading control. HRP-conjugated anti-rabbit IgG (Bio-Rad, 1706515, dilution 5000) and anti-mouse IgG (A4416, Sigma-Aldrich, dilution 1:10000) were used as secondary antibodies, respectively.

Immunofluorescence antibody staining

Anti-myosin IIA tail domain (M8064, Sigma-Aldrich, dilution 1:800), and 405 Alexa-Fluor-conjugated secondary antibodies (A31556, Molecular Probes, dilution 1:200). Cells were pre-fixed by addition of warm 2% PFA (Tousimis) into medium and subsequent 15 min incubation at room temperature. This was followed by fixation and permeabilization by 3.7% PFA, 0.2% glutaraldehyde and 0.25% Triton X-100 in PBS for 15 min. The fixed cells were then washed two times with PBS and blocked with 5% bovine serum albumin (BSA) for 30 min. The cells were then stained with primary antibodies overnight at 4 °C, and incubated with secondary antibodies for 1h at room temperature.

Drug treatment

For formin drug inhibition studies, cells were incubated with 20 or 40μM SMIFH2 (4401, TOCRIS, UK) in serum containing DMEM for 1-2h at 5% CO_2, 37 °C. In *in vitro* experiments, SMIFH2 (340316-62-3, Sigma-Aldrich) was used at a concentration of

100μM (see below). For myosin II inhibition studies, 30μM or 50μM Rho-kinase (ROCK) inhibitor Y27632 (Y0503, Sigma-Aldrich) or 20μM S-nitro-blebbistatin (13013-10, Cayman Chemicals, USA) was added for 10-20 min before the experiments or directly during observations. All inhibitors remained in the medium during the entire period of observation.

Optical tweezers and data acquisition

All experiments involving filopodia pulling were carried out on a Nikon A1R confocal microscope adapted for the use of laser tweezers. 2.19 μm diameter polystyrene beads (PC05N, Bangs Laboratories, USA) were coated with fibronectin (341635, Calbiochem, USA) according to a previous protocol (*73*). For bead trapping we used an infrared laser (λ = 1064nm, power 0.5-1W, YLM-5-LP-SC Ytterbium Fiber Laser, IPG photonics). The displacement of the beads from the center of the optical trap in confocal microscopy observations was monitored using piA640-210gm camera (Basler, Germany) at 0.5-1fps and Metamorph software for tracking. The smallest detectable bead displacement was ~5 nm, corresponding to the smallest force measured of ~0.04 pN. The trap stiffness was calibrated using the equipartition method (*74*) by tracking the fluctuations of a bead trapped by optical tweezers, using an Andor Neo sCMOS camera, at 100fps.

For laser trap experiments, HeLa-JW cells transfected by electroporation with GFP-myosin X and tdTomato-Ftractin, were seeded at a density of 2×10^4 cells ml^{-1} in 750μl onto chambered #1 borosilicate coverglasses (155383, Lab-Tek) coated with fibronectin (341635, Calbiochem, USA) by incubation in 1ng ml^{-1} solution in PBS for 20min at

37.0 °C. A reduced concentration of fibronectin (compared to that used for regular cell observations) was used to prevent the beads sticking to the cover slip. Chambers with cells were mounted on P-545.3R7 stage equipped with E-545 Plnano piezo controller (Physik Instrumente, Germany), which was moved in order to generate the pulling force between filopodia and trapped beads. The velocity of the stage movement was maintained in a range 10-20 nm/s by PIMikroMove 2.15.0.0 software. The specimen were incubated in a custom-built microscope hood at 37.0 °C, 5% CO_2 humidified environment. Simultaneously with pulling, the cells were imaged using lasers λ = 488nm and 561nm for excitation of GFP and tdTomato, respectively. Collected experimental data were processed by particle tracking algorithms of the Metamorph software.

***In vitro* assay for formin processivity in the presence of SMIFH2**

We used a microfluidics based assay to assess formin processivity in the course of formin-driven actin polymerization. The method has been described in more detail elsewhere (*56*). Briefly, formin construct Snap-mDia1(FH1FH2DAD)-6xHisTag was specifically anchored to the bottom surface of a microchamber, using a biotinylated pentaHis antibody (Qiagen) and streptavidin to bind to a biotin-BSA-functionalized glass surface which was further passivated with BSA. The microfluidics PDMS chamber height was 60 µm. Immobilized formin constructs were allowed to nucleate actin filaments by exposing them for 30s to a 2 µM solution of 20% Alexa488-labeled at Lys^{328} actin (*75*) and 0.4µM profilin in a buffer containing 10 mM Tris-HCl (Euromedex) pH 7.8, 1 mM MgCl2 (Merck) , 200 µM ATP (Roche) , 50 mM KCl (VWR Chemicals) and supplemented with 5 mM DTT (Euromedex), 1 mM DABCO (1,4-

diazabicyclo[2.2.2]octane) to reduce photobleaching. Recording of actin filament elongation was started after the buffer was changed to contain 1 μM unlabeled actin and 4 μM profilin, with or without 100 μM SMIFH2 (Sigma-Aldrich). The microfluidics flow was kept low enough to ensure that the viscous drag had no impact on filament detachment from formin. Images were acquired every 10 s on a Nikon Ti-E microscope using a 60x objective and a Hamamatsu Orca Flash 4.0 V2+ sCMOS camera. Actin was purified from rabbit muscle (*76*). Recombinant Profilin I and Snap-mDia1(FH1FH2DAD)-6xHisTag were expressed in *E. Coli* and purified (*77*).

Filopodia density and length measurement; tracking filopodia tips

Cells labeled with GFP-myosin X, tdTomato-Ftractin or mCherry-Utrophin were imaged in 488nm (green) and 594nm (red) channels, simultaneously. Cell segmentation was performed using an in-house algorithm implemented as a Fiji macro. The segmented cell was analyzed using MATLAB software CellGeo (*78*) to estimate filopodia density and their length. First, each data set, which corresponded to 10 frames per movie taken at 1-2 fps at x100, was averaged over time to generate a smooth image for each channel. The averaged images from the green and red channels were then summed to produce an enhanced image for segmentation. To optimize the segmentation results, filopodia segmentation and cell body segmentation was conducted in two separate steps. For filopodia segmentation, a background subtraction procedure with a rolling ball of 20-pixel radius was applied first, followed by Triangle auto-thresholding (Fiji Auto Threshold v1.16.1). For cell body segmentation, Gray Morphology open operator with a circle of 5-pixel radius was used (FiJi Morphology) to remove filopodia before applying

Li auto-thresholding (Fiji Auto Threshold v1.16.1). The final segmentation result was obtained by combining the masks from the above two steps. After segmentation, the BisectoGraph module of CellGeo (*78*) was used to partition each cell into the cell body and individual filopodia, based on the parameters called critical radius (roughly the half of maximal filopodia width) and minimum filopodia length. In our analysis, a critical radius of 0.7μm and a minimum filopodia length of 1.5μm were used. Note that, our definition of filopodia length slightly differed from that used in original paper by (*78*). Namely, in our analysis the filopodia length is defined to be the distance from the filopodia tip to the cell body boundary. The MATLAB code for computing this length was kindly provided by Dr. Tsygankov. For filopodia density quantification, the perimeter of the cell body was measured and the number of filopodia per unit of length (μm^{-1}) was computed.

To track the filopodia tips, the Imaris 8.3.1 spots tracking procedure was used. The filopodia tips were identified using segmentation procedure described above followed by MATLAB binary morphology function bwmorph with 'skel' and 'endpoints' operations.

Unconstrained filopodia elongation and shrinking rates were obtained by linear regression fitting of the filopodia tips trajectories at the regions corresponding to the periods of filopodia persistent growth or shrinking, respectively.

Supported lipid bilayer micro patterns chamber and filopodia tips trajectory analysis on rigid and fluid substrates

The cleaned glass coverslips were coated with PLL-g-PEG-biotin (Susos) for two hours followed by UV etching using 3 μm circular shape arrays of chromium (Cr) photomask (*79*), which resulted in removal of PLL-g-PEG-biotin polymers on the etched circular regions. After multiple rinses with UHQ water, phospholipid vesicles were introduced to the surface for 5 min, allowing the self-assembly of lipid bilayer on the etched glass surfaces. Phospholipid vesicles were synthesized using the existing protocol (*79*). Specifically, 98 % of DOPC (1,2-dioleoyl-sn-glycero-3-phosphocholine) was mixed with 2 % of biotin-DOGC (1,2-dioleoylsn-glycero-3-[(N-(5-amino-1-carboxypentyl)iminodiacetic acid)-succinyl]) biotin lipids. The lipid solution was further diluted with Tris buffered saline (TBS, Sigma-Aldrich) at a ratio of 1:1 before introduction. The glass coverslips were assembled into the donut shape chamber at the UHQ water reservoir. The hybrid substrate was then incubated with 0.1 % bovine serum albumin (BSA, Sigma Aldrich) for two hours to reduce non-specific protein absorption. Next, 1 μg/ml of Dylight-405 NeutrAvidin (Thermo Fisher) was introduced to the chamber for one hour, and then incubated with 1ug/ml of RGD-biotin (Peptides International) for one hour. Multiple rinses with UHQ were applied after each step. A fluidity test of RGD molecules at the surface of supported lipid bilayer (SLB) was performed by fluorescence recovery after photobleaching. The concentration of RGD on both SLB and PLL-g-PEG polymer was similar, based on the estimated fluorescence of Dylight-405 NeutrAvidin (Fig. S8).

HeLa cells expressing a myosinX-GFP chimera were introduced to the chamber, allowing cells to adhere to and spread on the RGD-coated hybrid substrate. Cells were visualized

using a charge coupled EMCCD camera (Photometrics) coupled with total internal reflection microscopy (TIRF) with 100x objective (1.5 NA, Nikon). The chamber was maintained at 37 ^{o}C during observation. The time-lapse video was recorded at varying intervals over a range of 3 – 5 s.

The GFP-Myosin X cluster at the filopodia tip was tracked by using a cross-correlation single particle tracking method (*80*). Obtained trajectories were analyzed using the "inpolygon" matlab function to find trajectory segments that crossed SLB circular islands and computer drawn islands in the center of the SLB pattern. The time intervals between the initial and end points of the segments were then used to estimate the average filopodia tip dwell time on the SLB and computer drawn circular islands. In addition, the ratio between the number of filopodia tip trajectories remaining inside rigid and fluid circles relatively to the total number of trajectories in the circles during the period of observation was calculated to characterize the filopodia adhesion preferences to rigid and fluid substrates (Fig. 6). In this analysis, we used only trajectories that spanned more than 5 frames.

Statistics and reproducibility

Prism (GraphPad 6.0 Software) was used for statistical analysis. Each exact n value is indicated in the corresponding figure or figure legend. The significance of the differences (*P* value) was calculated using the two-tailed unpaired Student's *t*-test.

Figure S1

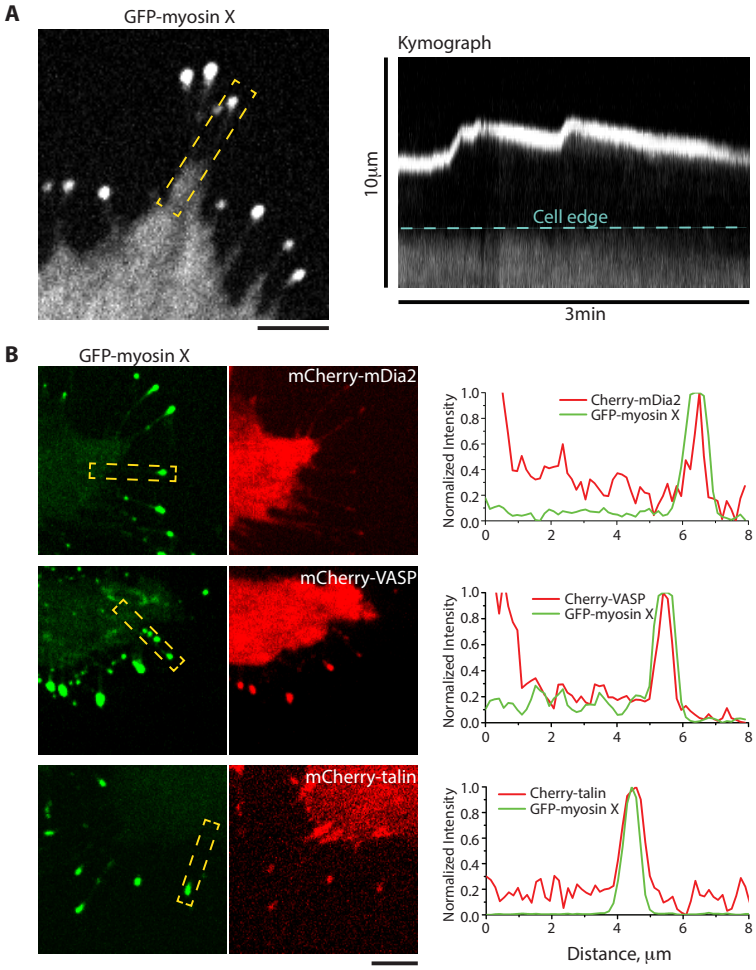
A
GFP-myosin X
Kymograph
10μm
Cell edge
3min
B
GFP-myosin X
mCherry-mDia2
mCherry-VASP
mCherry-talin
Cherry-mDia2
GFP-myosin X
Cherry-VASP
GFP-myosin X
Cherry-talin
GFP-myosin X
Normalized Intensity
Distance, μm
C
Fibronectin
Talin
Integrin
Formin
Actin filament
VASP
Myosin X

Fig. S1.

Dynamics and composition of filopodia induced by myosin X expression

(A) Left: Filopodia from HeLa-JW cells expressing GFP-myosin X. Myosin X positive "comet tails" are seen at the tips of filopodia. Right: a kymograph showing the growth of a GFP-myosin X labeled filopodium indicated by dashed box in the left image. Note that periods of fast growth alternate with periods of slow shrinking. **(B)** Filopodia tips labeled with myosin X are enriched with mDia2, VASP and talin. Left: Images of filopodia in cells co-expressing GFP-myosin X with mCherry fusion constructs of mDia2, VASP and talin respectively. Right: line scans of the fluorescence intensities through the filopodia indicated by dashed boxes in the left images. Intensities of the myosin X, mDia2, VASP and formin were normalized to their maximal values at the filopodia tips. Scale bars, 5μm. **(C)** A cartoon depicting the protein complex at the tip of filopodium. Actin filaments connected with integrin receptors via talin and polymerized by formin family and VASP proteins located at the tip. Myosin X is interacting with actin filaments, integrins and VASP.

Figure S2

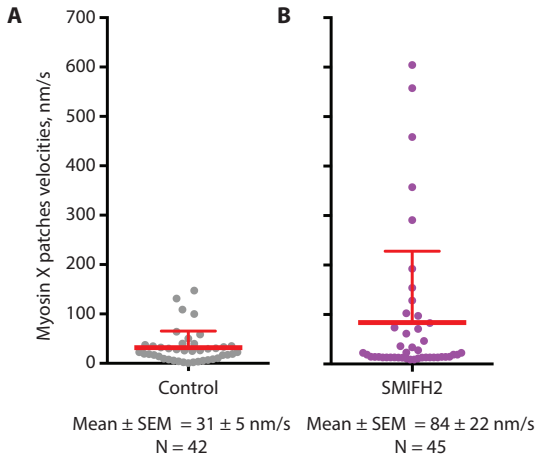
A
B
Myosin X patches velocities, nm/s
700
600
500
400
300
200
100
0
Control
SMIFH2
Mean ± SEM = 31 ± 5 nm/s
N = 42
Mean ± SEM = 84 ± 22 nm/s
N = 45

Fig. S2

Retrograde intra-filopodial movement of myosin X patches in control and SMIFH2 treated cells

The velocities of intra-filopodial movement of myosin X patches were measured in untreated control cells **(A)** and in cells treated with 20μM SMIFH2 for 2 hours **(B)**. The cells were filmed for about 10-20 min, with measurements performed only on filopodia that demonstrated movement of myosin X. In control cells, measurements were performed on filopodia after the bead had attached to the filopodia tip, since filopodia that were not attached to a bead seldom contained centripetally moving myosin X patches. In cells pre-treated with SMIFH2, measurements were performed in filopodia that were not attached to beads as centripetally moving myosin X patches were always visible. Each symbol corresponds to the velocity of a single myosin X patch. Means are indicated by thick horizontal lines in both graphs. The error bars correspond to SD values.

Experimental data were collected from 11 filopodia in 6 cells and 6 filopodia in 6 cells for control and SMIFH2 treated cells, respectively.

Figure S3

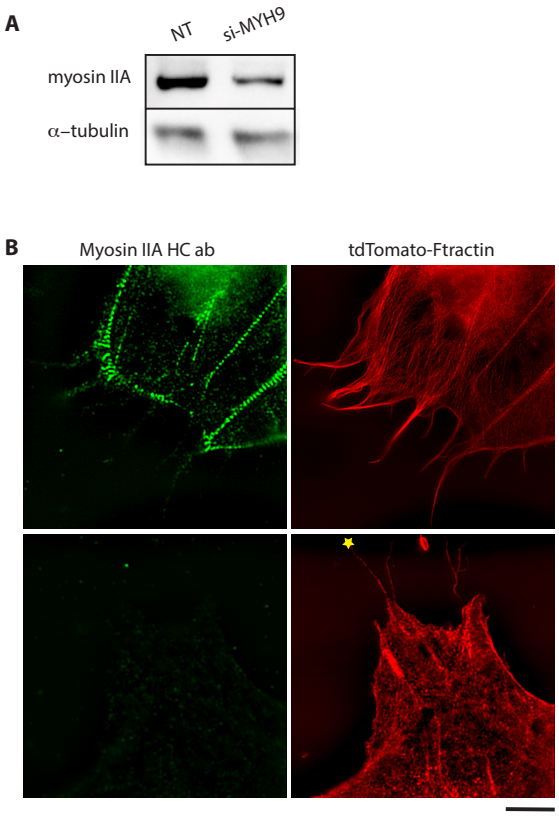
A
NT
si-MYH9
myosin IIA
α–tubulin
B
Myosin IIA HC ab
tdTomato-Ftractin

Fig. S3

siRNA knockdown of myosinIIA

(A) Immunoblots of myosin IIA in non-targeted and knockdown cells. α-tubulin was used as loading control. **(B)** Control cells (transfected with a non-targeting siRNA pool) displayed typical myosin II filament stacks, as visualized by N-SIM microscopy after immunofluorescence staining with an antibody against myosin IIA heavy chain tail domain (left). The stacks were associated with either straight actin fibers, or actin bundles delineating the cell boundary, as visualized by the expression of tdTomato-Ftractin (right). Numerous actin-containing filopodia were induced by myosin X expression (not shown). **(C)** The myosin knockdown cell (one of the cells used in the pulling experiments) did not contain either myosin IIA (left) or prominent actin stress fibers (right), but still contained filopodia. The filopodium attached to the bead is indicated by asterisk. Scale bars, 10μm.

Figure S4

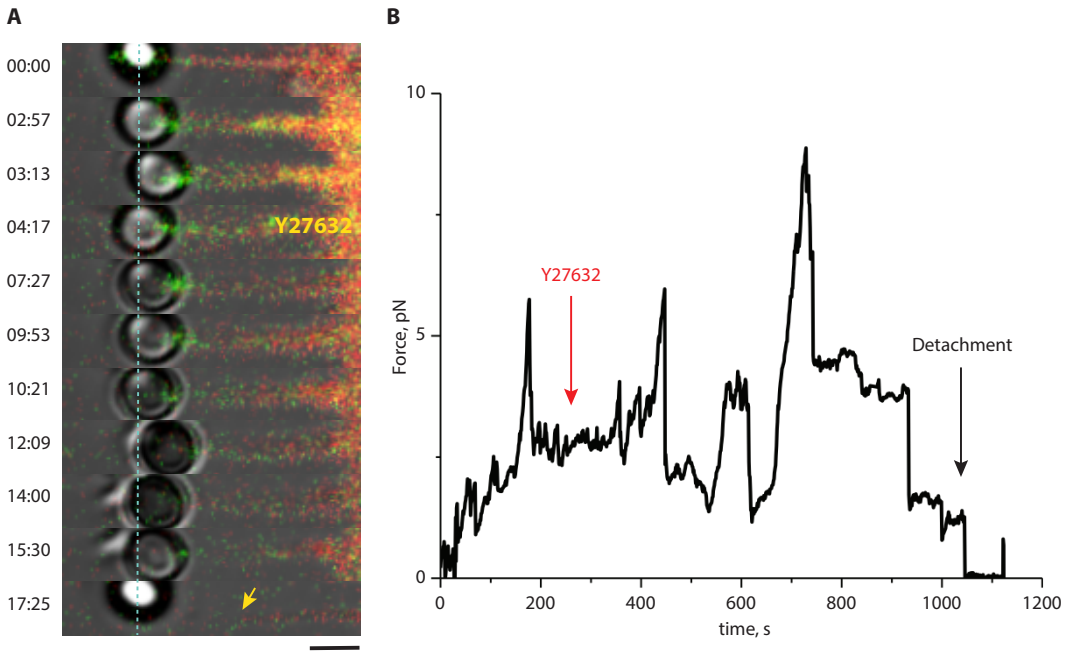
A
00:00
02:57
03:13
04:17
07:27
09:53
10:21
12:09
14:00
15:30
17:25
Y27632
B
10
5
0
Force, pN
Y27632
Detachment
0
200
400
600
800
1000
1200
time, s

Fig. S4

Effect of ROCK inhibitor, Y27632, on force-induced filopodia growth and adhesion

A fibronectin-coated bead, which was trapped by laser tweezers, was attached to the filopodia tip. Filopodia growth was then induced through the generation of pulling force, which resulted from the movement of the microscope stage, as in Fig. 1. At about 4 min following the start of the stage movement, 30μM of Y27632 was added, and this resulted in bead detachment at about 17 min. The position of the trapped bead during filopodia growth is shown in **(A)**. Deflections of the bead position from the trap axis were used to calculate the forces exerted by filopodia on the bead **(B)**. Scale bar, 2μm.

Figure S5

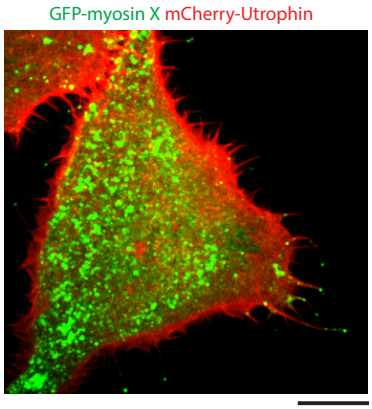

Fig. S5

Effect of formin inhibitor SMIFH2 on myosin X induced filopodia

A cell, labeled with GFP-myosin X and Cherry-Utrophin, was treated with 20μM SMIFH2 formin inhibitor for 2 hours**.** Note that the majority of the filopodia do not contain myosin X. Scale bar, 10μm.

Figure S6

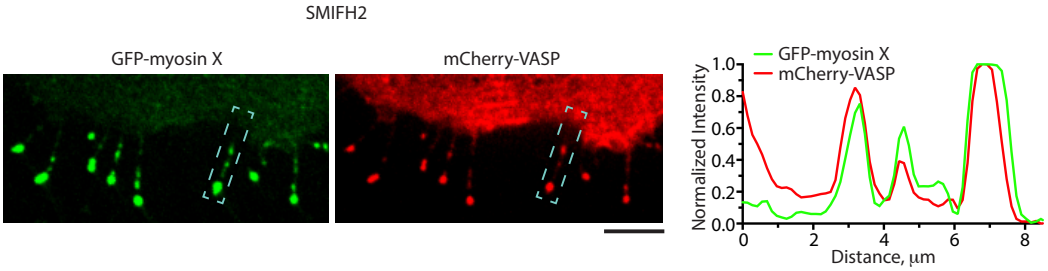
SMIFH2
GFP-myosin X
mCherry-VASP
GFP-myosin X
mCherry-VASP
Normalized Intensity
1.0
0.8
0.6
0.4
0.2
0.0
0
2
4
6
8
Distance, μm

Fig. S6

Localization of VASP at myosin X patches in cells treated with formin inhibitor

Distribution of GFP-myosin X (green, left panel) and Cherry-VASP (red, central panel) in the same cell 1.5h after the addition of 20μM SMIFH2. Right panel: the line scans through the boxed area, showing the co-distribution of myosin X and VASP. Fluorescent intensities are normalized to their maximal values. Scale bars, 5μm.

Figure S7

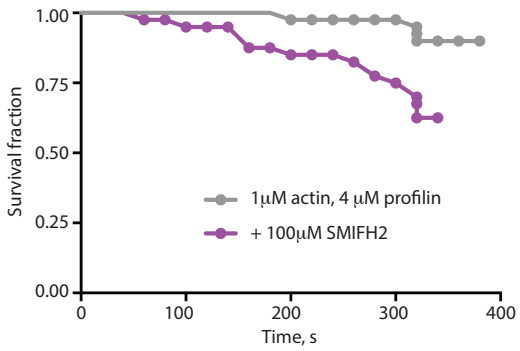
1.00
0.75
0.50
0.25
0.00
Survival fraction
0
100
200
300
400
Time, s
1μM actin, 4 μM profilin
+ 100μM SMIFH2

Fig. S7

SMIFH2 enhances the detachment of formins from actin filaments in vitro

The constitutively active mDia1 formin construct (FH1FH2DAD) was anchored to the glass surface of a microfluidic chamber by one of their FH2 domains using an anti-His antibody (as in Jegou et al. 2013, see Materials and Methods). Once the formin had nucleated a filament, it was exposed, from time zero onward, to 1μM actin and 4μM profilin, in absence or presence of 100μM SMIFH2. The time at which each filament detached from its formin was recorded. SMIFH2 enhanced this detachment by 1 order of magnitude without affecting the formin mediated elongation rates of the filaments (35 ± 6 vs. 32 ± 8 subunits/s, n = 40 filaments without and with SMIFH2, respectively).

Figure S8

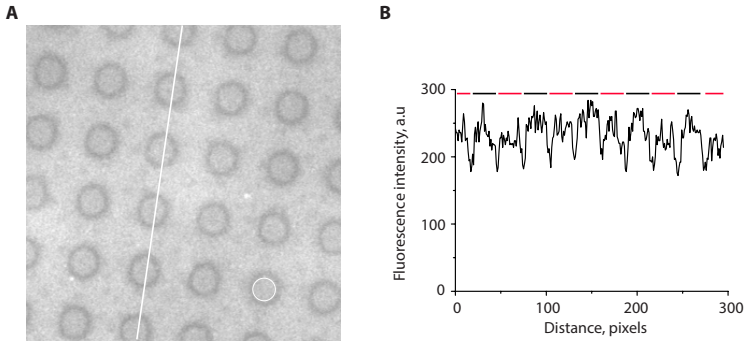
A
B
300
200
100
0
0
100
200
300
Fluorescence intensity, a.u
Distance, pixels

Fig. S8.

(A) A fluorescence image of a hybrid substrate containing a RGD ligand which is tethered to PLL-PEG polymer (background) and a supported lipid bilayer (SLB) surface (circles) via a biotin- Dylight-405 NeutrAvidin conjugation. **(B)** The line intensity profile along the white line in (A). The red and black lines at the top of the curve mark the SLB and PLL-PEG regions, respectively, showing a similar concentration of RGD ligands in both regions.

Movie S1

Dynamics of filopodia induced by myosin X expression

Growing, pausing and retracting filopodia in HeLa-JW cells overexpressing GFP-myosin X. The myosin X is localized to filopodia tips where it appears as characteristic "comet tails". The duration of the entire movie is 3 min, the movie images were recorded at 4.31 frames per second (fps) and display rate is 50 fps. The time (min:s) is indicated using the "Time stamper" plugin in ImageJ.

Movie S2

Dynamics of pulling-driven growth of GFP-myosin X-induced filopodia

Sustained filopodial growth was induced by pulling force generated through the movement of a microscope stage. The tip of the filopodium was attached to a laser trapped fibronectin-coated bead. The experimental set up is depicted in Fig. 2A. The frames from this movie, and the kymograph based on it, are shown in Fig. 2B and 2C respectively. The duration of the entire movie is 26 min 52 s. Movie images were recorded at 0.5 fps and displayed at 25 fps.

Movie S3

Pulling of GFP-myosin X-induced filopodia with concanavalin A-coated beads

Pulling force was applied to a filopodium attached to a cocanavalin-A-coated laser trapped bead by moving the microscope stage. This force was applied to induce filopodia growth, but in contrast with the results obtained from experiments using fibronectin-coated beads (supplementary movie 2), under these conditions, filopodium did not grow

and formation of notable membrane tethers (visible after 8 min in the movie) occurred instead. The duration of the movie is 14 min 58 s and the movie images were recorded at 0.5 fps with a display rate of 15 fps.

Movie S4

Disappearance of myosin II filaments associated with filopodium upon cell treatment with Y27632

HeLa-JW cells were transfected with labeled myosin II regulatory light chain (GFP-RLC) to visualize myosin II filaments, and mApple-myosin X to visualize filopodia tips. In addition to numerous myosin II filaments in the cell body, few filaments, appearing as doublets of fluorescent dots, were observed at the base of filopodium. Addition of the ROCK inhibitor Y27632 resulted in the gradual disappearance of myosin II filaments, including the filaments associated with the filopodium. Frames from this movie were shown in Fig. 3B. The duration of the entire movie is 28 min 52 s and the movie images were recorded at 0.05 fps with a display rate of 7 fps.

Movies S5A, B, C and D

Inhibition of myosin II or formin suppresses filopodia adhesion (see also Fig. 4 A-D)

(A) Pulling force induced sustained growth of a filopodium in a control cell. The experiment was analogous to that described in the legend to supplementary movie 2. The cell was used as a control for experiments with inhibitors presented in Fig. 4. The duration of the movie is 17 min 8 s. (B) Effect of light-insensitive blebbistatin. The cell was pretreated with 20μM S-nitro-blebbistatin for 10-20 min prior to placing the laser

trapped fibronectin-coated bead onto the filopodium tip. 30 s later, stage movement commenced simultaneously with filming. Note that adhesion of the bead to filopodium was broken 6 min 44 s after starting the stage movement. The duration of the movie is 13 min 12 s. (C) Effect of myosin IIA knockdown. The detachment of the filopodium from the bead occurred 3 min 50 s after stage movement was initiated. The velocity of the movement of myosin X patches observed in this experiment was significantly lower then the velocity of myosin II driven movement (Fig. 6, supplementary movie 8). The duration of the movie is 4 min 38 s. (D) Effect of formin inhibition by SMIFH2. The cell was pretreated with 40μM SMIFH2 for 1 hour prior the bead being placed onto a filopodium tip. To check whether the bead had attached to the filopodium, the laser trap was switched off for several s, during which time unattached beads disappeared from the field of view. The detachment of the filopodium from the bead occurred about 2 min after stage movement was initiated. The duration of the entire movie is 4 min 56 s. All the movies in this figure were recorded at 0.5 fps with a display rate of 15 fps.

Movie S6

Effect of ROCK inhibitor, Y27632, on force-induced filopodia growth and adhesion

This movie corresponds to the frames shown in supplementary Fig. 2. Filopodia growth was induced by applying a pulling force, generated as a result of microscope stage movement, as in Fig.2. At about 4 min after stage movement commenced, 50μM of Y27632 was added, which eventually resulted in bead detachment at 17 min. The duration of the entire movie is 19 min 22 s. The movie was recorded at 1 fps and displayed at 25 fps.

Movie S7

Effect of formin inhibition on dynamics of myosin X in filopodia

This movie corresponds to the Fig. 5C. The filopodia were induced by cell transfection with a construct encoding GFP-myosin X. Before imaging, the cell was treated with 20μM of SMIFH2 for 2 hours. Note the apparent disintegration of the myosin X containing patch at the tip of filopodia into numerous small patches, the majority of which rapidly moved centripetally from the filopodium tip into the cell body (sometimes interrupted by short periods of anterograde movement towards the tip). The duration of the entire movie is 5 min; the movie was recorded at 4 fps and displayed at 100 fps.

Movie S8A-C

Effect of myosin II inhibition on fast centripetal movement of myosin X patches in filopodia of SMIFH2 treated cells

These movies correspond to Fig.6. A cell transfected with GFP-myosin X was filmed before treatment (A), 15 min after the addition of 20μM SMIFH2 (B) and 20 min after the subsequent addition of 30μM Y27632 (C). Note that after SMIFH2 was added, myosin X comet tails underwent rapid disintegration into small patches, which moved centripetally towards the cell body (B). Addition of Y27632 resulted in cessation of this movement (C). The duration of the movies A-C were 6 min 41 s; the movie images were recorded at 0.1 fps and displayed at 7 fps.

Movie S9. Filopodia distinguish between fluid and rigid substrates. GFP-myosin X transfected HeLa JW cell spreading on the micropatterned substrate with 3um islands covered with supported lipid bilayer (SLB). Both the islands and the substrate between them were coated with fluorescent Dylight-405 RGD ligand shown in blue. The GFP-myosin X positive filopodia tips are shown in green. The movie started 30 min following the cell plating. Note that filopodia tips apparently avoid the SLB islands, see the analysis in Fig. 6. The duration of the movies was 16 min 40 s; the movie images were recorded at 0.3 fps and displayed at 30 fps.